

Effects of Be on the II–VI/GaAs interface and on CdSe quantum dot formation

S. P. Guo,^{a)} X. Zhou, O. Maksimov, and M. C. Tamargo^{b)}

New York State Center for Advanced Technology on Photonic Materials and Applications, Center for Analysis of Structures and Interfaces (CASI), Department of Chemistry, City College-CUNY, New York, New York 10031

C. Chi, A. Couzis, and C. Maldarelli

Department of Chemical Engineering, City College-CUNY, New York, New York 10031

Igor L. Kuskovsky and G. F. Neumark

School of Mines and Department of Applied Physics, Columbia University, New York, New York 10027

(Received 7 January 2001; accepted 7 June 2001)

The effects of Be on the II–VI/GaAs interface and on CdSe quantum dot (QD) formation were investigated. A (1×2) surface reconstruction was observed after a Be–Zn coirradiation of the (001) GaAs (2×4) surface. ZnBeSe epilayers grown after the Be–Zn coirradiation show very high crystalline quality with x-ray rocking curve linewidths down to 23 arcsec and a low etch pit density of $4 \times 10^4 \text{ cm}^{-2}$, and good optical quality with a band-edge photoluminescence (PL) emission peak linewidth of 2.5 meV at 13 K. However, ZnBeSe epilayers grown after Zn irradiation alone have poor crystalline quality and poor optical properties. Atomic force microscopy measurements show that CdSe QDs grown on ZnBeSe have higher density and smaller size than those grown on ZnSe. A narrower PL emission peak with higher emission energy was observed for the CdSe QDs sandwiched by ZnBeSe. These results indicate that the formation of CdSe QDs as well as the II–VI/GaAs interface are modified by the presence of Be. © 2001 American Vacuum Society. [DOI: 10.1116/1.1388209]

I. INTRODUCTION

Self-assembled quantum dots (QDs) are of great interest due to the low dimensional physical phenomena they present as well as their high potential for novel device applications. So far, most of the investigations have involved III–V systems, such as (In, Ga)As/GaAs,^{1–3} InP/InGaP,⁴ and GaSb/GaAs,⁵ which are suited for near infrared range applications. Much less work has been done in II–VI systems, which are attractive for optoelectronic applications in the blue-green spectral regions. CdSe QDs grown on ZnSe and ZnMnSe have been reported.^{6,7} These uncapped CdSe QDs are relatively large and exhibit intermixing with the underlying layer. Furthermore, they are unstable and a ripening behavior has been observed.⁶

Another extremely important issue for the growth of II–VI materials, typically grown on III–V substrates, is the II–VI/III–V interface quality. In the case of the growth of ZnSe-based materials on GaAs, it is important to avoid any tendency to form a Se- (2×1) surface reconstruction on the GaAs surface.⁸ On such a surface, isolated islands are easily formed, and very high density of stacking faults are produced. This is believed to be related to the formation of Ga₂Se₃ at the interface.

Beryllium chalcogenides have a high degree of covalent bonding compared to other wide gap II–VI semiconductors.⁹ High crystalline quality ZnBeSe alloys have been successfully grown by molecular beam epitaxy (MBE) using a few

monolayers (MLs) of BeTe as a buffer layer.¹⁰ High quality ZnBeSe has also been obtained by using a Be–Zn coirradiation of GaAs surface, in which the GaAs buffer layer surface was exposed to a combined Be and Zn flux for 20 s before initiating the growth of ZnBeSe.¹¹ The change of the surface conditions by adding Be and the expected higher bonding energy for Be alloys may be the reasons for the high quality. In view of the pronounced effect of Be treatment of II–VI/III–V interface on the ZnBeSe quality, one might expect that Be may also affect the formation of CdSe QDs. Here we present our results of effects of Be on the II–VI/GaAs interface and on CdSe QD formation. A (1×2) surface reconstruction was observed after a Be–Zn coirradiation of the GaAs (001) surface. ZnBeSe epilayers grown with the Be–Zn coirradiation show much higher crystalline quality and better optical properties than those grown with a Zn irradiation alone. Atomic force microscopy (AFM) and photoluminescence (PL) measurements show that the formation of CdSe QDs is also modified by the presence of Be on the surface.

II. EXPERIMENT

All the samples were grown by MBE on GaAs (001) substrates in a dual chamber Riber 2300 system, which has a III–V growth chamber and a II–VI growth chamber connected by ultrahigh vacuum (UHV). For QD formation, in order to achieve a flat growth front, a 200 nm GaAs buffer layer, 30 periods of (2 nm GaAs/2 nm AlAs) short-period superlattice and a 30 nm GaAs layer were grown at 580 °C in the III–V chamber after the deoxidization of GaAs substrate

^{a)}Current address: EMCORE Corp., 394 Elizabeth Ave., Somerset, NJ 08873; electronic mail: shipping_guo@emcore.com

^{b)}Electronic mail: tamar@sci.cuny.edu

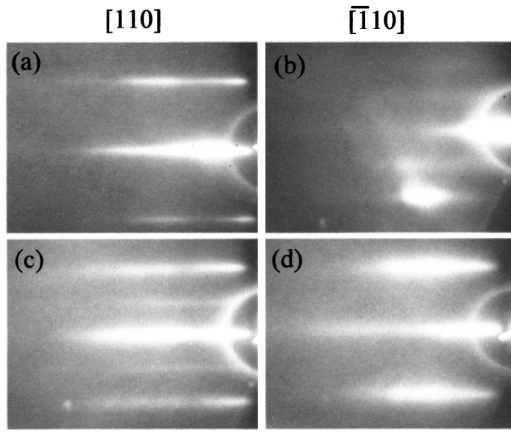


FIG. 1. RHEED patterns of the GaAs (001) surface after the Be–Zn coirradiation [(a) and (b)] and of the ZnBeSe (001) surface grown under Se-rich conditions [(c) and (d)] along $[110]$ and $[\bar{1}10]$ azimuths.

under an As flux. Then the substrate with III–V buffer layers was transferred into the II–VI chamber in UHV. Prior to the growth of II–VI epilayers, a Be–Zn coirradiation of the GaAs surface was performed at 170°C to avoid the formation of Ga_2Se_3 , which is believed to be related to the formation of stacking faults.⁸ Once the substrate with the buffer layer was transferred to the II–VI chamber, the main shutter was opened immediately for 20 s (the Zn and Be shutters were already open). For the Zn-irradiation case, the GaAs surface was exposed to a Zn flux only, with the Be shutter closed.¹¹ Then the substrate temperature was increased to 250°C and a 6 nm ZnSe buffer layer was grown. After this $\text{Zn}_{0.97}\text{Be}_{0.03}\text{Se}$ (or ZnSe) epilayers, which are nearly lattice matched to GaAs, were grown at 270°C . CdSe QDs were formed by depositing 2.5 MLs of CdSe on ZnBeSe (or ZnSe) surface with a substrate temperature ranging from 250 to 380°C and with a growth interruption of 30 s. For PL measurement a 100 nm ZnBeSe (or ZnSe) top barrier was grown to confine the carries in the QDs.

Reflection high-energy electron diffraction (RHEED) was used for *in situ* monitoring of the growth process and AFM was used for *ex situ* characterization of the surface morphology. The crystalline quality and Be concentration were assessed by double crystal x-ray diffraction (DCXRD) measurements using $\text{Cu } K_{\alpha 1}$ radiation. Etch pit density (EPD) measurements were carried out using either 0.2% Br_2/MeOH at room temperature or 32% HCl solutions at 60°C .¹¹ PL measurements were performed at 13 and 77 K using the 325 nm line of a He–Cd laser for excitation.

III. RESULTS AND DISCUSSION

A. Effects of Be on the II–VI/GaAs interface

Figures 1(a) and 1(b) show RHEED patterns of the GaAs (001) surface after the Be–Zn coirradiation along $[110]$ and $[\bar{1}10]$ azimuths. Since we closed the main shutter in the III–V chamber at 550°C after the GaAs buffer layer growth, the RHEED pattern remains a typical GaAs (2×4) surface reconstruction before the Be–Zn coirradiation. After the

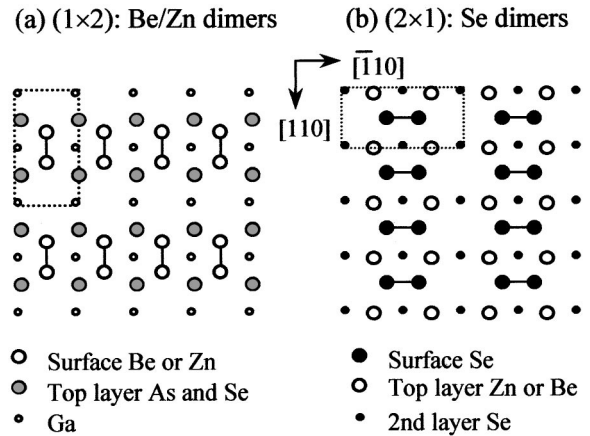


FIG. 2. Structure models of a (1×2) GaAs (001) surface with Be/Zn dimers after the Be/Zn coirradiation (a) and of a (2×1) ZnBeSe (001) surface with Se dimers grown under Se-rich conditions (b).

Be–Zn coirradiation of the GaAs surface, a stable (1×2) RHEED pattern was observed. Such a (1×2) surface reconstruction is not observed on the GaAs (2×4) surface exposed only to a Zn flux (Zn irradiation). In that case, the RHEED pattern remains (2×4) , although slightly diffuse, after the Zn irradiation. On the other hand, a (2×1) Se exposed GaAs (001) surface has been previously observed and it has been shown to be due to the formation of a full ML of Se dimers along the $[\bar{1}10]$ direction.⁸ Analogous to this, we propose that the observed (1×2) surface reconstruction is most likely due to the formation of a full ML of Be/Zn dimers along the $[110]$ direction. Figure 2(a) shows a proposed structure model of such a (1×2) surface. This structure is one of several possibilities that arise when electron-counting rules are applied to satisfy the bonding of the surface atoms. Which of these surfaces is most likely to form and how they are actually formed during growth is difficult to predict and is beyond the scope of this article. A (1×2) surface reconstruction on Zn terminated ZnSe (001) surface based on Zn dimers along the $[110]$ direction has also been proposed,¹² but has not been previously observed by experiments during MBE growth of ZnSe-based materials. ZnSe (001) surface under Zn-rich growth conditions typically exhibits a $c(2\times 2)$ surface reconstruction which has been shown to be related to the formation of a half ML of Zn atoms on the surface¹³ while the ZnSe (001) surface under Se-rich growth conditions usually exhibits a (2×1) surface reconstruction (associated with Se dimers along the $[\bar{1}10]$ direction).⁸ The absence of a (1×2) surface reconstruction on the Zn-irradiated GaAs (001) surface as well as on the Zn-terminated ZnSe (001) surface during MBE growth suggests that stable Zn dimers do not form on either surface, since most of the Zn atoms reevaporate under typical growth conditions due to the low bonding energy of Zn–As bonds and Zn–Zn bonds. However, beryllium compounds in general have a high degree of covalent bonding so that Be atoms are expected to bond more strongly to the GaAs surface, thus enabling the Be/Zn dimers to form.

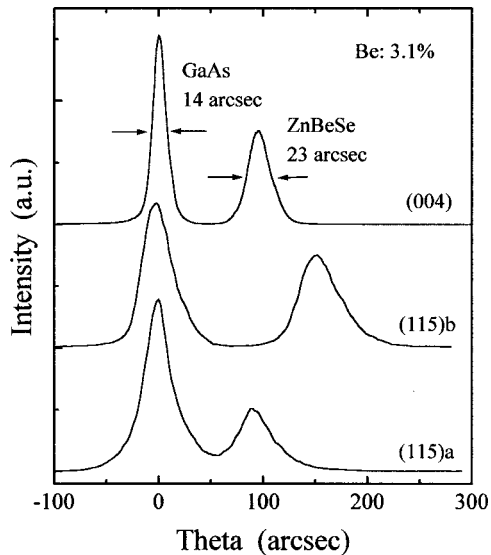


FIG. 3. (004) symmetrical reflection and (115)*a* and *b* asymmetrical reflection DCXRD rocking curves for a ZnBeSe epilayer grown with the Be–Zn coirradiation.

Once growth of ZnBeSe is initiated the surface transforms to a typical (2×1) reconstruction for group VI-rich growth of II–VI compounds. Figures 1(c) and 1(d) show the typical (2×1) RHEED patterns along $[110]$ and $[\bar{1}10]$ azimuths for the ZnBeSe surface grown under Se-rich growth conditions. This surface reconstruction is similar to that of the ZnSe surface grown under Se-rich conditions. A structure model of the (2×1) ZnBeSe surface is shown in Fig. 2(b), where a full ML of Se dimers is proposed to form on the ZnBeSe surface along the $[\bar{1}10]$ direction, similar to that for ZnSe.⁸

Figure 3 shows the (004) symmetrical reflection and the (115)*a* and *b* asymmetrical reflection DCXRD rocking curves for a 1.4- μm -thick ZnBeSe epilayer grown with the Be–Zn coirradiation. A very narrow peak related to the ZnBeSe epilayer, with a full width at half maximum (FWHM) of 23 arcsec, was observed, indicating an extremely high crystalline quality. The EPD for the epilayer is $4 \times 10^4 \text{ cm}^{-2}$ (shown in Table I), confirming the high quality of ZnBeSe epilayer. From the (115)*a* and *b* asymmetrical reflection DCXRD we can obtain the perpendicular and parallel lattice constant: a_1 and a_2 . The bulk lattice constant then is calculated from the equation

$$a = a_1 \{ 1 - [2\nu / (1 + \nu)] [(a_1 - a_2) / a_1] \}.$$

Here ν is the Poisson's ratio (we use the value of ν for ZnSe of 0.28 for the ZnBeSe because of the small Be concentration). Assuming that Vegard's law is valid for ZnBeSe

TABLE I. Properties of ZnBeSe epilayers.

II–VI/III–V interface treatments	FWHM of DCXRC (arcsec)	EPD (cm^{-2})	FWHM of PL 13 K (meV)
Be–Zn coirradiation	23	4×10^4	2.5
Zn irradiation alone	>300	$>10^6$	5

and using a_{ZnSe} of 5.6676 Å and a_{BeSe} of 5.139 Å, the Be concentration of 3.1% can be assessed from the lattice constant.

The FWHM of the x-ray rocking curve for ZnBeSe grown with Zn irradiation alone is very broad, and the layer has a high EPD (data are shown in Table I) although the Be concentration is very close to that of the layer grown with the Be–Zn coirradiation. The difference between two cases is only the treatment of the II–VI/GaAs interface. This suggests that Be atoms at the interface can effectively suppress the interaction of Se atoms with Ga atoms, and the formation of Ga_2Se_3 , which is believed to be related to the formation of stack faults.⁸ The narrow PL emission linewidth of 2.5 meV at 13 K for the ZnBeSe epilayer grown with the Be–Zn coirradiation, is half of that grown with the Zn irradiation alone (shown in Table I). This indicates that ZnBeSe epilayers grown with the Be–Zn coirradiation also have much better optical properties compared to layers grown with Zn irradiation alone. It should be noted that when ZnSe growth on GaAs is performed with Zn irradiation alone (without the Be cell on) it produces high quality layers.¹⁴ During the growth of ZnBeSe, excess heating of the surface due to the thermal irradiation from the high temperature Be cell ($\sim 900^\circ\text{C}$) appears to diminish the effectiveness of the Zn-irradiation process. Under these conditions simultaneous exposure with Be and Zn (i.e., Be–Zn coirradiation) is required.

B. Effects of Be on CdSe QD formation

AFM measurements of CdSe QDs grown on ZnBeSe and ZnSe were performed at room temperature. A smooth surface for the ZnBeSe surface without CdSe was observed with a surface roughness of about 4 nm. When 2.5 MLs of CdSe was deposited on the ZnBeSe at the various growth temperatures we studied (250–380 °C), CdSe QDs were formed. The QD density and size depend on the growth temperature. Figure 4(a) shows a $(2 \mu\text{m} \times 2 \mu\text{m})$ AMF image of 2.5 MLs of CdSe deposited on ZnBeSe at 320 °C. The average QD density is $1.5 \times 10^9 \text{ cm}^{-2}$ with an average diameter of ~ 70 nm and an average height of ~ 12 nm. The three-dimensional AFM image of this sample is shown in Fig. 5. It can be seen that the CdSe QDs have a spherical shape. For comparison, an AFM image of 2.5 MLs of CdSe deposited on ZnSe at 320 °C is shown in Fig. 4(b). To ensure that the surface conditions (i.e., surface temperature) in the two experiments are the same, except for the presence of Be in the ZnBeSe layers, the Be cell was kept on ($\sim 900^\circ\text{C}$) during both growth sequences. Much lower QD density and larger QD size than those grown on ZnBeSe under the same conditions were observed on ZnSe. The average QD density is $5 \times 10^8 \text{ cm}^{-2}$ with an average diameter of ~ 105 nm and an average height of ~ 18 nm. The higher density and smaller size of the CdSe QDs grown on ZnBeSe suggests that the properties of the surface (i.e., surface free energy) are modified by the presence of Be. Very recently, this behavior has also been observed by Keim *et al.*,¹⁵ who demonstrated that coverage of the ZnSe starting surface with a fractional ML of BeSe (0.01–0.05 ML) leads to enhanced CdSe island forma-

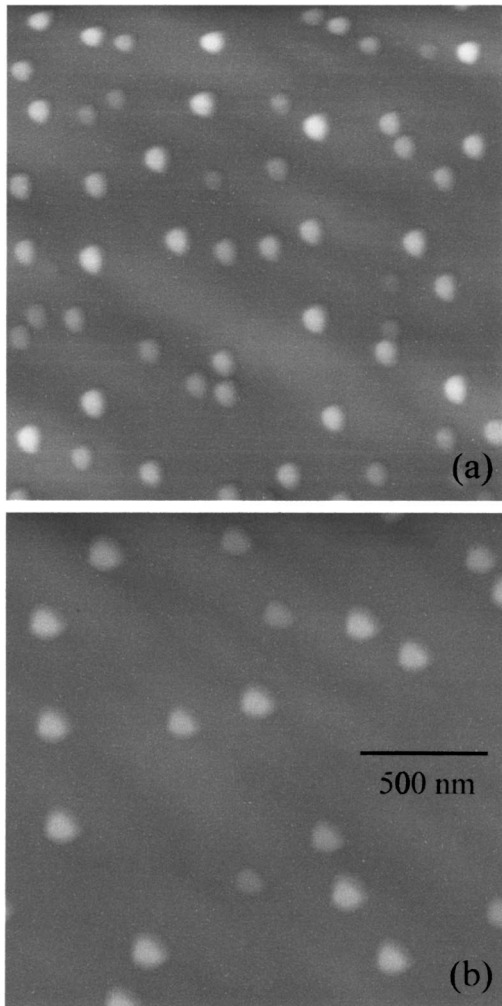


FIG. 4. AMF images of 2.5 MLs of CdSe deposited on ZnBeSe (a) and on ZnSe (b) at 320 °C ($2\ \mu\text{m} \times 2\ \mu\text{m}$).

tion in CdSe/ZnSe heterostructures well below the CdSe thickness of 0.6–0.7 ML, whereas 2.1 MLs of CdSe are required to form CdSe QDs on the ZnSe surface.¹⁶ The QD size observed in our study is slightly larger than the previously reported data.⁶ Further optimization of growth conditions, such as Se/Cd flux ratio and postgrowth annealing process, should be pursued. Nevertheless the comparison between the two systems should still be valid.

Figure 6 shows the PL spectra of CdSe QDs with 2.5 MLs of CdSe sandwiched by ZnBeSe (a) and by ZnSe (b) at 77 K. A strong blue-green emission peak at 2.418 eV with FWHM of 49 meV was observed for the CdSe QDs sandwiched by ZnBeSe and an emission peak at 2.372 eV with FWHM of 56 meV was observed for the CdSe QDs sandwiched by ZnSe. These values are similar to the previous reports of CdSe QDs embedded between ZnSe layers.^{6,16} The narrower FWHM for CdSe QDs sandwiched by ZnBeSe compared to that of QDs sandwiched by ZnSe may be due to the higher uniformity of QD size in the ZnBeSe case. The higher emission peak energy in the ZnBeSe case is believed to be related to the smaller QD size with higher quantum confinement and the slightly higher barrier energy due to the presence of Be in

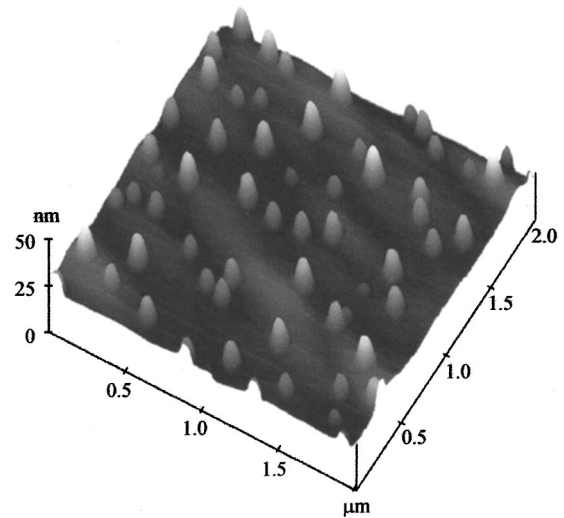


FIG. 5. Three-dimensional AFM image of 2.5 MLs of CdSe deposited on ZnBeSe at 320 °C ($2\ \mu\text{m} \times 2\ \mu\text{m}$).

ZnBeSe. The observation of a significant effect on the CdSe QD size and density by such a small concentration of Be ($\sim 3\%$) suggests that higher Be content in the barrier layer may further decrease the QD size as well as increase the quantum confinement.

IV. CONCLUSIONS

In summary, effects of Be on the II–VI/GaAs interface and on CdSe QD formation were investigated. A (1×2) surface reconstruction was observed after the Be–Zn coirradiation of the (001) GaAs surface, whereas the (2×4) surface reconstruction remains for Zn irradiation alone. We attribute the observed stable (1×2) surface reconstruction to the formation of a full ML of Be/Zn dimers along the $[110]$ direction. ZnBeSe epilayers grown with the Be–Zn coirradiation show very high crystalline quality with x-ray rocking curve linewidths down to 23 arcsec and a low EPD of 4

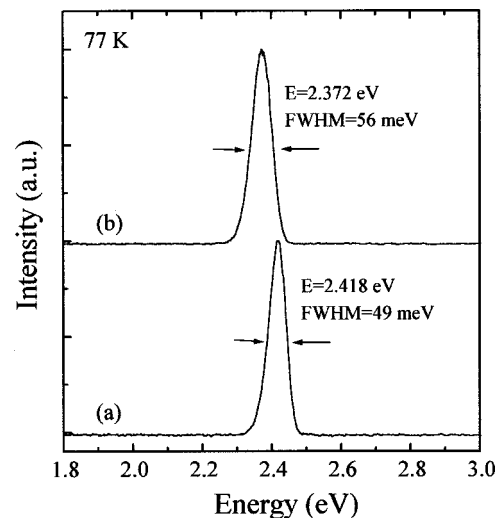


FIG. 6. PL spectra of CdSe QDs with 2.5 MLs of CdSe sandwiched by ZnBeSe (a) and by ZnSe (b) at 77 K.

$\times 10^4 \text{ cm}^{-2}$, as well as good optical properties with FWHM of the band-edge PL emission peak of 2.5 meV at 13 K. By contrast, ZnBeSe epilayers grown with Zn irradiation alone have poor crystalline quality and poor optical properties. AFM measurements show that CdSe QDs grown on ZnBeSe have higher density and smaller size than those grown on ZnSe. The average QD density is $1.5 \times 10^9 \text{ cm}^{-2}$ with an average diameter of ~ 70 nm and an average height of ~ 12 nm for CdSe QDs with 2.5 MLs of CdSe deposited on ZnBeSe at 320 °C. A narrower PL emission peak with higher emission energy was observed for the CdSe QDs grown on ZnBeSe compared to those grown on ZnSe. These results indicate that the formation of CdSe QDs as well as the II–VI/GaAs interface are modified by the presence of Be.

ACKNOWLEDGMENT

The authors acknowledge the support of the National Science Foundation under Grant No. DMR9805760.

¹D. Leonard, M. Krishnamurthy, S. Fafard, J. M. Merz, and P. M. Petroff, *J. Vac. Sci. Technol. B* **12**, 1063 (1994).

²A. Madhukar, Q. Xie, P. Chen, and A. Konkar, *Appl. Phys. Lett.* **64**, 2727 (1994).

³S. Fafard, D. Leonard, J. L. Merz, and P. M. Petroff, *Appl. Phys. Lett.* **65**, 1388 (1994).

⁴A. Kurtenbach, E. Eberl, and T. Shitara, *Appl. Phys. Lett.* **66**, 361 (1995).

⁵F. Hatami, N. N. Ledentsov, M. Grundmann, J. Böhrer, F. Heinrichsdorff, M. Beer, D. Bimberg, S. S. Ruvimov, P. Werner, U. Gosele, J. Heydenreich, U. Richter, S. V. Ivanov, B. Y. Meltser, P. S. Kop'ev, and Z. Alferov, *Appl. Phys. Lett.* **67**, 656 (1995).

⁶S. H. Xin, P. D. Wang, A. Yin, C. Kim, M. Dobrowolska, J. L. Merz, and J. K. Furdyna, *Appl. Phys. Lett.* **69**, 3884 (1996).

⁷F. Flack, V. Nikitin, P. A. Crowell, J. Shi, J. Levy, N. Samarth, and D. D. Awschalom, *Phys. Rev. B* **54**, R17312 (1996).

⁸D. Li and M. D. Pashley, *J. Vac. Sci. Technol. B* **12**, 2547 (1994).

⁹F. Fischer, Th. Litz, H. J. Lugauer, U. Zehnder, Th. Gerhard, W. Ossau, A. Waag, and G. Landwehr, *J. Cryst. Growth* **175/176**, 619 (1997).

¹⁰F. Fischer, M. Keller, T. Gerhard, T. Behr, T. Litz, H. J. Lugauer, M. Keim, G. Reuscher, T. Baron, A. Waag, and G. Landwehr, *J. Appl. Phys.* **84**, 1650 (1998).

¹¹S. P. Guo, Y. Luo, W. Lin, O. Maksimov, M. C. Tamargo, I. Kuskovsky, C. Tian, and G. F. Neumark, *J. Cryst. Growth* **208**, 205 (2000).

¹²A. García and J. E. Northrup, *J. Vac. Sci. Technol. B* **12**, 2678 (1994).

¹³H. H. Farrell, M. C. Tamargo, and S. M. Shibli, *J. Vac. Sci. Technol. B* **8**, 884 (1990).

¹⁴C. C. Chu, T. B. Ng, J. Han, G. C. Hua, R. L. Gunshor, E. Ho, E. L. Warlick, L. A. Kolodziejski, and A. V. Nurmikko, *Appl. Phys. Lett.* **69**, 602 (1996).

¹⁵M. Keim, M. Korn, J. Seufert, G. Bacher, A. Forchel, G. Landwehr, S. Ivanov, S. Sorokin, A. A. Sitnikova, T. V. Shubina, A. Toropov, and A. Waag, *J. Appl. Phys.* **88**, 7051 (2000).

¹⁶D. Schikora, S. Schwedhelm, D. J. As, K. Lischka, D. Litvinov, A. Rosenauer, D. Gerthsen, M. Strassburg, A. Hoffmann, and D. Bimberg, *Appl. Phys. Lett.* **76**, 418 (2000).